Unveiling Amplified Isolation in Climate Networks due to Global Warming

Yifan Cheng[1], Panjie Qiao[1]*, Meiyi Hou[2], Yuan Chen[1], Wenqi Liu[1] and Yongwen Zhang[1]*

[1.] Data Science Research Center, Faculty of Science, Kunming University of Science and Technology, Kunming 650500, China；

[2.] Department of Atmospheric Sciences, Yunnan University, Kunming, China.

Correspondence to: Panjie Qiao(qiaopanjie0720@163.com), and Yongwen Zhang (zhangyongwen77@gmail.com)

Abstract

Our study utilizes global reanalysis of near-surface daily air temperature data, spanning from 1949 to 2019, to construct climate networks. By employing community detection for each year, we reveal the evolving community structure of the climate network within the context of global warming. Our findings indicate significant changes in measures such as the network modularity and the number of communities, over the past 30 years. Notably, the community structure of the climate network undergoes a discernible transition since the early 1980s. We attribute this transition to the substantial increase in isolated nodes, primarily concentrated in tropical ocean regions. Additionally, we demonstrate that nodes experiencing amplified isolation tend to diminish connectivity with other nodes globally, particularly those within the same tropical oceanic basin, while showing a significant strengthening of teleconnection with the Eurasian and North African continents. The amplified isolation in the climate network could be associated with the weakening of tropical circulations such as

the Hadley cell and the Walker circulation in response to increasing greenhouse gases.

Key words： *Climate network, community detection, modularity, isolated nodes.*

1 Introduction

Since the 20th century, with the continuous increase of greenhouse gas emissions, the global climate system is undergoing warming (IPCC, 2023; Christopher et al., 2012; Hallegatte et al., 2011; Hunt and Watkiss, 2011). Global warming has led to a significant increase in various extreme weather events, encompassing extreme heatwaves, cold spells, heavy precipitation, droughts, and severe hurricanes etc. (Doney et al., 2009, Mondal et al., 2021, Konapala et al,. 2020, Mukherjee et al., 2020). In addition, it has a serious impact on global air quality, food production, energy consumption, transportation, water resources, economic and ecosystems, etc. (Thomas et al., 2004; Salehyan and Hendrix, 2014; Nordhaus and William D., 2017; Burke et al., 2015). Global warming has triggered significant transformations in atmospheric circulation and ocean circulation patterns, impacting the dynamics of the Earth's climate system (Shepherd, T., 2014; Vecchi, Gabriel A. and Brian J. Soden, 2007). The rise in global temperatures is a key driver of alterations in atmospheric circulation patterns, especially in the tropical belt, influencing phenomena such as the Hadley Cell, Walker Circulation, and the Madden-Julian oscillation (Lu et al., 2007; Tokinaga et al., 2012; Hu et al., 2021; Chang et al., 2015). The expansion of the tropics and changes in the distribution of sea surface temperatures contribute to shifts in the intensity and frequency of tropical cyclones and the behavior of the El Niño-Southern Oscillation (ENSO) (Emanuel et al., 2005; Kossin et al., 2020; Cai et al., 2021). These modifications in tropical circulations have widespread implications for precipitation patterns, extreme weather events, and regional climate variability. Additionally, the Atlantic Meridional Overturning Circulation (AMOC) may undergo a transition, with potential collapse having severe impacts on the

climate in the North Atlantic and European regions (Rahmstorf et al., 2015; Boers, 2021). Previous studies have argued that the global climate experienced a shift in the 1970s (Graham, 1994; Tsonis et al., 2007; Swanson et al., 2009). Understanding these systematic changes is imperative for predicting future climate scenarios (e.g., precipitation, temperature, wind) and formulating effective adaptation and mitigation strategies.

Faced with these climatic systematic changes, the adoption of complex network analysis has become increasingly essential in the realm of climate science. The climate system is intricately complex, marked by multivariable and multiscale nonlinear dynamics. Unveiling the internal structure of the climate system necessitates the application of sound research methods. Complex network analysis emerges as a potent tool for investigating the nonlinear dynamics and structural characteristics of complex systems (Newman, 2018; Zou et al., 2019). Over the past several years, complex network methodologies have gained widespread application in the realm of climate science. In the climate network, nodes represent geographical locations where time series data for temperature (or other climate variables) are accessible. Links are established through bivariate similarity measures such as correlation, mutual information, or event synchronization between these time series (Tsonis et al., 2004; Donges et al., 2009; Quiroga et al., 2002). Climate network techniques have proven effective in enhancing our understanding of various climate and weather phenomena, including ENSO, teleconnection patterns of weather, and atmospheric pollution (Tsonis et al., 2008; Yamasaki et al., 2008; Fan et al., 2017; Kittel et al., 2021; Zhou et al., 2015; Boers et al., 2019; Di Capua et al., 2020; Zhang et al., 2019). Notably, complex network analysis has unveiled the weakening of tropical circulation under global warming (Geng et al., 2021; Fan et al., 2018). Furthermore, these techniques

have demonstrated utility in forecasting climate events (Boers et al., 2014; Ludescher et al., 2014; Meng et al., 2018; Ludescher et al., 2021).

Complex systems naturally exhibit partitioning into multiple modules or communities, a significant feature of complex networks (Palla et al., 2005). In the context of climate networks, each community serves as a representation of a climate subsystem, shedding light on the interrelationships between different components (Tsonis et al. 2011). Community detection algorithms, rooted in modularity maximization (Newman, 2006; Cherifi et al., 2019), have been pivotal in unveiling structures within climate networks. These algorithms have successfully identified community structures in diverse contexts, including rainfall networks (Agarwal et al., 2018), interaction networks of sea surface temperature observations (Tantet et al., 2014), global climate responses to ENSO phases (Kittel et al., 2021) and the quantification of climate indices. Yet, scant attention has been given to the impact of global warming on the community structure of climate networks, particularly those with small sizes. This research endeavors to employ network analysis and community detection to investigate how global warming is reshaping the structure of the global temperature network. The ultimate goal is to deepen our understanding of climate change and inform strategies for addressing its impacts.

Therefore, based on the near-surface temperature structure climate network, this paper studies the impact of global warming on climate network. Employing the Louvain community detection algorithm, it analyzes the evolution of network topology and reveals the underlying factors driving changes in the network structure. The main structure of this paper is as follows: Section 2 introduces the data and methods; Section 3 discusses the evolution of climate network topology in the context of global warming; Section 4 summarizes the results.

2 Data

This study utilizes daily air temperature reanalysis data from the National Centers for Environmental Prediction (NCEP) and the National Center for Atmospheric Research (NCAR) at a resolution of $2.5° \times 2.5°$, spanning the near-surface (sig995 level) temperatures from 1949 to 2019. The dataset comprises 10,512 grid points over the global. We select 726 nodes to construct the network and maintain the spatial density homogeneity within the climate network nodes in the sphere as suggested in previous studies (Zhou et al., 2015; Guez et al., 2014). These nodes are strategically spaced to ensure uniform coverage of the Earth in Euclidean space, as depicted in Supplementary Figure S1(a). The nodes are equally distributed, with distances between any two neighboring nodes approximately 850 km, as illustrated in Supplementary Figure S1(b).

3 Methods

3.1 Constructing the climate network

Climate networks are constructed based on the near-surface air temperature data for each year from 1949 to 2019, resulting in a total of 71 established climate networks. The time series of a node (denoted as i) undergoes deseasonalization by subtracting the average seasonal cycle and dividing by the standard deviation of the cycle, resulting in the temperature anomaly (denoted as $T_i^y(t)$, where y is the index of year)(Fan et al.,2018). To obtain the link strength between each pair of nodes i and j, we then calculate the time-lagged cross-correlation function(Fan et al., 2021):

$$C_{i,j}^{y}(-\tau) = \frac{\langle T_i^y(t) T_j^y(t-\tau)\rangle - \langle T_i^y(t)\rangle \langle T_j^y(t-\tau)\rangle}{\sqrt{\langle (T_i^y(t) - \langle T_i^y(t)\rangle)^2\rangle} \cdot \sqrt{\langle (T_j^y(t-\tau) - \langle T_j^y(t-\tau)\rangle)^2\rangle}}, \quad (1)$$

$$C_{i,j}^{y}(\tau) = \frac{\langle T_i^y(t-\tau) T_j^y(t)\rangle - \langle T_i^y(t-\tau)\rangle \langle T_j^y(t)\rangle}{\sqrt{\langle (T_i^y(t-\tau) - \langle T_i^y(t-\tau)\rangle)^2\rangle} \cdot \sqrt{\langle (T_j^y(t) - \langle T_j^y(t)\rangle)^2\rangle}}, \quad (2)$$

where $\langle\,\rangle$ denotes the mean value, based on which $\langle f(a)\rangle = \frac{1}{365}\sum_{t=1}^{365} f(t-a)$; t represents time and the time lag is denoted as $\tau \in [0,200]$ days.

Therefore, the link strength between each pair of nodes in the network is denoted as follows:

$$W_{i,j}^{y} = \frac{max\left(C_{i,j}^{y}(\tau)\right) - mean\left(C_{i,j}^{y}(\tau)\right)}{std\left(C_{i,j}^{y}(\tau)\right)}, \quad (3)$$

in this context, "max","mean" and "std" denote the maximum value, mean, and standard deviation of the cross-correlation over all time lags from -200 to 200 days between nodes i and j. Strong autocorrelation can inflate the significance of cross-correlation. In contrast, the link strength $W_{i,j}^{y}$ is more effective in mitigating the effects of autocorrelation, offering a more reasonable reflection of the relationship between two nodes (Guez et al., 2014). This approach has proven valuable in predicting climate phenomena (Ludescher et al., 2021). To select meaningful links in the network and eliminate false associations, we retain the top 5% of links in the network such that a threshold of $\theta = 3.5$ (corresponding to a p-value of 0.03 (Palus et al., 2011) signifying that 97% of the values in the shuffled data fall below this threshold in Supplementary Figure S2) is applied to obtain an adjacency matrix A (when $W_{i,j}^{y} \geq \theta$, the element $A_{ij} = 1$, otherwise, the element $A_{ij} = 0$).

3.2 Community Detection

Subsequently, the obtained sequence of climate networks underwent community detection using the Louvain community detection algorithm. The key steps of this method involve traversing each node in the network and attempting to relocate it to a neighboring node in a different community to optimize the modularity Q. If moving a node to another community increases the modularity, the move is executed; otherwise, it remains unchanged. In other words, the process assesses whether the increment in modularity ΔQ resulting from the move is positive, and this procedure is repeated until no further node movements are possible. Here is the formula for calculating modularity(Blondel et al., 2008):

$$Q = \frac{1}{2m}\sum_{i,j}\left[A_{ij} - \frac{k_i k_j}{2m}\right]\delta(c_i, c_j), \quad (4)$$

where $k_i = \sum_j A_{ij}$ and $k_j = \sum_i A_{ij}$ ($i \neq j$) are the number of links connected to vertex (node) i and j, c_i represents the community to which node i belongs, $\delta(\mu, v)$ equals 1 if $\mu = v$, otherwise 0, and $m = \frac{1}{2}\sum_{ij} A_{ij}$. Modularity has become a metric for assessing the quality of community divisions, with high modularity indicating strong internal connections within a community and weaker connections with other communities.

4 Results

In order to investigate the evolution of the network's topology in the context of global warming, we construct the network for each year from 1949 to 2019 and apply community detection to the network. In Figure 1(a), we show that the network modularity for the early years (1949-1981) is largely below the average level. While in the recent years (1982-2019), the network modularity remain consistently above the average level. There is a significant transition in the modularity around 1982. Supplementary Figure S3 illustrates the modularity values obtained by four distinct algorithms, as outlined in Ref (Kittel et al., 2021). The results highlight the robustness of the modularity transition around 1982 across different algorithms. Notably, the Louvain algorithm produces the highest modularity values, indicating its superior effectiveness in identifying community structures. The number of communities and modularity exhibit similar evolutionary patterns as shown in Figure 1(b). Although the trend in the change of the number of communities is not as pronounced as the trend in network modularity, it is still evident that the number of communities was mostly below the average level in the first 33 years, while in the recent 38 years, the majority of community numbers are above the average level (as shown in Figure 1(b)). Figure 1(c) also shows the escalating count of isolated nodes since 1982. The isolated node is identified by the Louvain algorithm with a community size of 1 (equivalent to a degree of zero, $k_i = 0$). The observed systematic change in community structure since

the early 1980s could be linked to the reported climate shift, as indicated by Refs (Graham, 1994; Tsonis et al., 2007; Swanson, 2009) utilizing both reanalysis data and climate simulations. The substantial increase in greenhouse gas emissions has contributed to a shift in the mean climate state since the 1980s in the tropical belt (Cai et al., 2021). This shift is further evident in the altered properties of El Niño since the early 1980s (Gan et al., 2023).

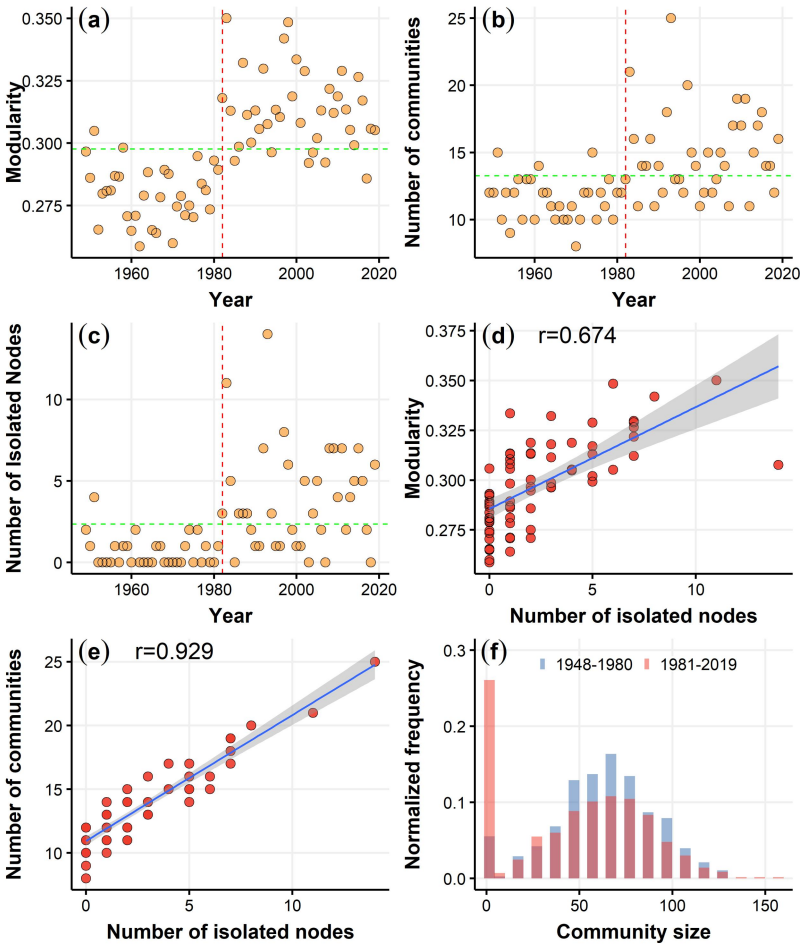

Figure 1: Temporal evolution of (a) network modularity, (b) the number of communities and (c) the number of isolated nodes from 1949 to 2019, illustrated by the green dashed line denoting the average level, and the red dashed line represents the transition around 1982. Scatter plot of (d) the network modularity, (e) the number of communities versus the number of isolated nodes during the period 1949-2019. (f) The normalized frequencies of community size for 1949-1981 and 1982-2019 respectively (normalized by the total number of communities for each period), where the first bar represents the normalized frequency of the community with a node.

Since 1982, the number of communities has been on the rise. This trend appears to be closely linked to

the increasing count of isolated nodes. We observe the relationship between modularity and the number of isolated nodes and find a strong positive correlation with a correlation coefficient of 0.674 (as shown in Figure 1(d)). The high correlation with network modularity indicates that the trend in the number of isolated nodes is consistent with changes in the network's topological structure. Furthermore, from Figure 1(e), we observe that the correlation between the number of isolated nodes and the number of communities reaches 0.929. The high correlation with the number of communities suggests that the overall increase in the number of communities is driven by the increase in isolated nodes. To further strengthen the verification of whether the changes in the number of communities and network modularity since 1982 are related to the number of isolated nodes. We examine represents the normalized frequency of community sizes in 1949-1981 and 1982-2019 (as shown in Figure 1(f)). There are two peaks for the isolated node and the community with size around 60 for both 1949-1981 and 1982-2019. In 1949-1981, the proportion of isolated nodes in the overall community is not prominent. However, in 1982-2019, the proportion of isolated nodes has dramatically increased and has become the largest component in the community distribution. Therefore, the transition in modularity and the number of communities since 1982 can be attributed to the substantial increase in the number of isolated nodes.

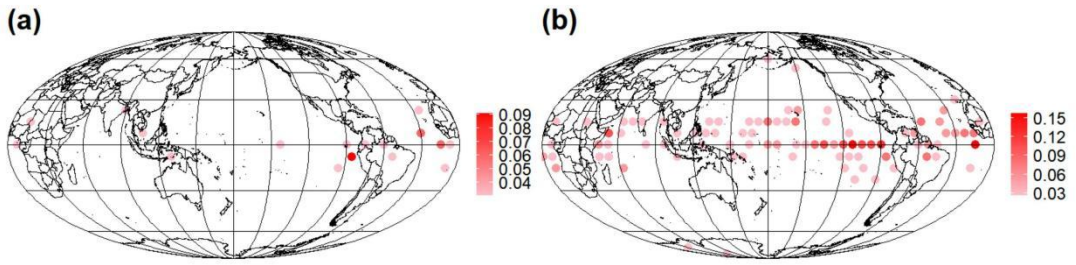

Figure 2: Occurrence probability maps of isolated nodes for (a) 1949-1981, and (b) 1982-2019.

Next, we will further study the relationship between changes in climate network structure and isolated nodes. The occurrence probability maps of isolated nodes for 1949-1981 and 1982-2019 are shown in Figure 2. From 1949 to 1981, few isolated nodes are mainly distributed in the Equatorial East Pacific and Equatorial Atlantic oceans, with a low occurrence probability. However, from 1982 to 2019,

189 the isolated nodes with higher occurrence probabilities can appear almost everywhere in the equatorial
190 regions such that the total number of communities increase. The occurrence probability of isolated
191 nodes in the last 38 years is not only higher than the first 33 years but also covers a larger area than the
192 first 33 years. Hence, isolated nodes in the equatorial region have been systematically increasing since
193 the early 1980s, resulting in changes to the climate network structure. To establish robustness, we
194 conduct the analysis using different community detection algorithms, the maximum time lag of 365
195 days, the shuffled nodes and a 6-month shift for the time window. The obtained results are consistent,
196 as illustrated in Supplementary Figures. S3-S12.

197 To gain a deeper understanding and verify how the isolation in climate networks is amplified in
198 the Equatorial regions, we select three nodes with the highest frequency of isolation in three regions:
199 the Indian Ocean, the Pacific Ocean, and the Atlantic Ocean, respectively. We study the relationships
200 between the three nodes and other nodes across the climate network structure. Specifically, we
201 calculate the probability of the selected node and each of other 725 nodes belonging to the same
202 community for time periods 1949-1981 and 1982-2019, and compute the difference the two time
203 periods. This probability can reflect which important region responds to the amplified isolation of the
204 selected node.

205 In Figure 3(a), for 1949-1981, the selected Indian Ocean node exhibits high probability with
206 surrounding nodes belonging to the same community. However, for the 1982-2019 in Figure 3(b), this
207 probability is weakened, particularly in their association with the oceanic regions. the difference of the
208 probability between 1982-2019 and 1949-1981 is shown in Figure 3(c). Blue (red) points in Figure 3(c)
209 represent the decreased (increased) probability with time. In general, most areas have decreased
210 probability. Still, some areas i.e., the Eurasian and North Africa continent have increased probability to

connect to the selected Indian Ocean node.

Since the 1980s, the probabilities of the nodes in the Pacific and the equatorial Pacific region belonging to the same community are noticeably diminished (as shown in Figure 4). Examining the probability map of the selected Atlantic Ocean node and other global nodes belonging to the same community in Figure 5, it is observed a similar behavior. The selected three high-frequency isolated nodes are surrounded by relatively strong connectivity regions during the first 33 years. However, these regions experience varying degrees of weakening in connectivity during the subsequent 38 years. It is worth noting that since the 1980s, the connectivity between high-frequency isolated nodes in the Indian Ocean, Atlantic Ocean, and Pacific Ocean with global oceanic regions is diminishing, especially the strength of their connections with their respective oceanic regions significantly decreasing. However, the association with the Eurasian and North Africa continent is strengthening. Previous studies have suggested the weakening of tropical circulations such as the Hadley cell and the Walker circulation, in response to increasing greenhouse gases (Lu et al., 2007; Tokinaga et al., 2012; Cai et al., 2021). The weakened tropical circulations can be associated with reduced link strength, a decrease in the number of links, leading to a subsequent increase in the number of isolated nodes. To further illustrate this phenomenon, we present the averaged strength (W) and the number of links over the tropical Pacific Ocean, Indian Ocean, and Atlantic Ocean as functions of years in Supplementary Figure S13, which indeed indicates significantly decreasing trends in the averaged strength (W) and the number of links for these oceans. Additionally, the weakened tropical circulation could potentially trigger extreme climate phenomena, such as the intensification of El Niño, with more pronounced teleconnection impacts on distant regions (Fan et al., 2017 ; Hu et al., 2021). This could, in turn, strengthen the linkage between equatorial regions and continents in climate networks.

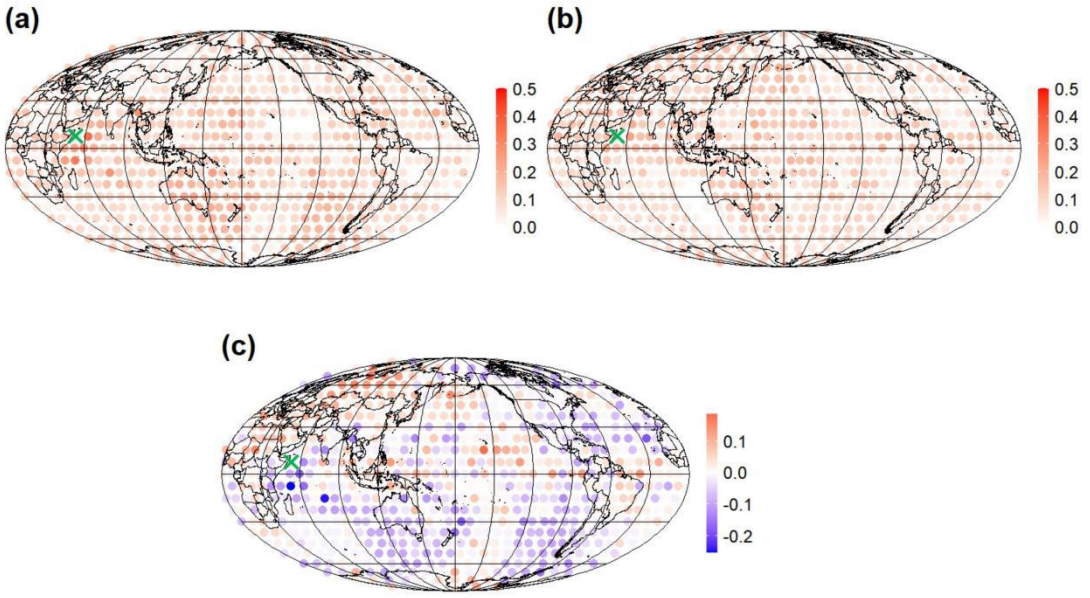

233

234 **Figure 3: Probability maps of the Indian Ocean node and other global nodes belonging to the same**

235 **community for (a) 1949-1981, (b) 1982-2019, and (c) the difference of the probability between 1982-2019 and**

236 **1949-1981. The symbol of cyan cross represents the selected Indian Ocean node.**

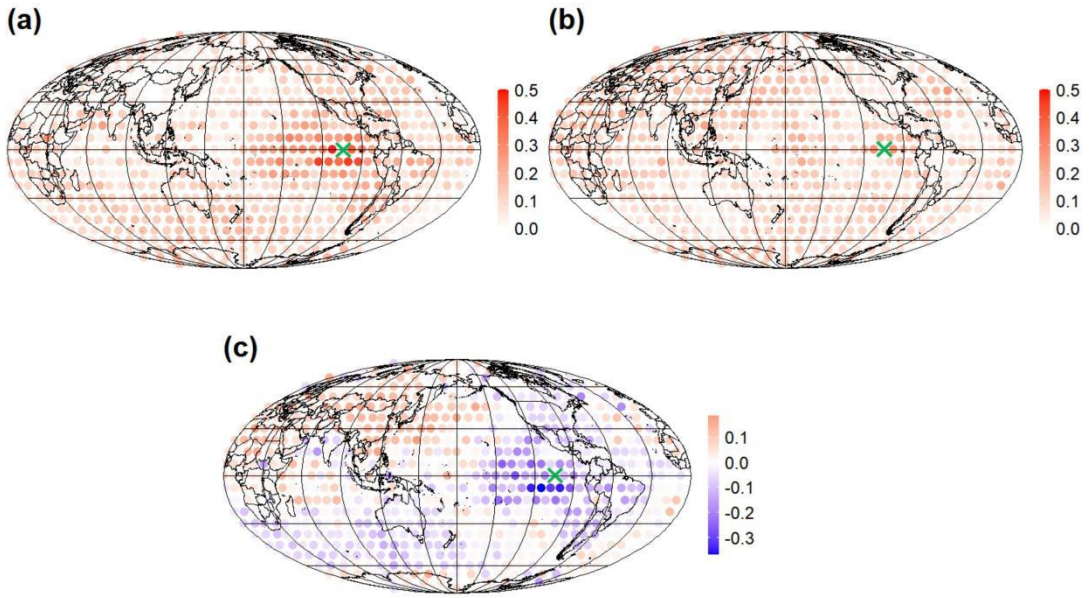

237

238 **Figure 4: Probability maps of the Eastern Pacific Ocean node and other global nodes belonging to the same**

239 **community for (a) 1949-1981, (b) 1982-2019, and (c) the difference of the probability between 1982-2019 and**

240 **1949-1981. The symbol of cyan cross represents the selected Eastern Pacific Ocean node.**

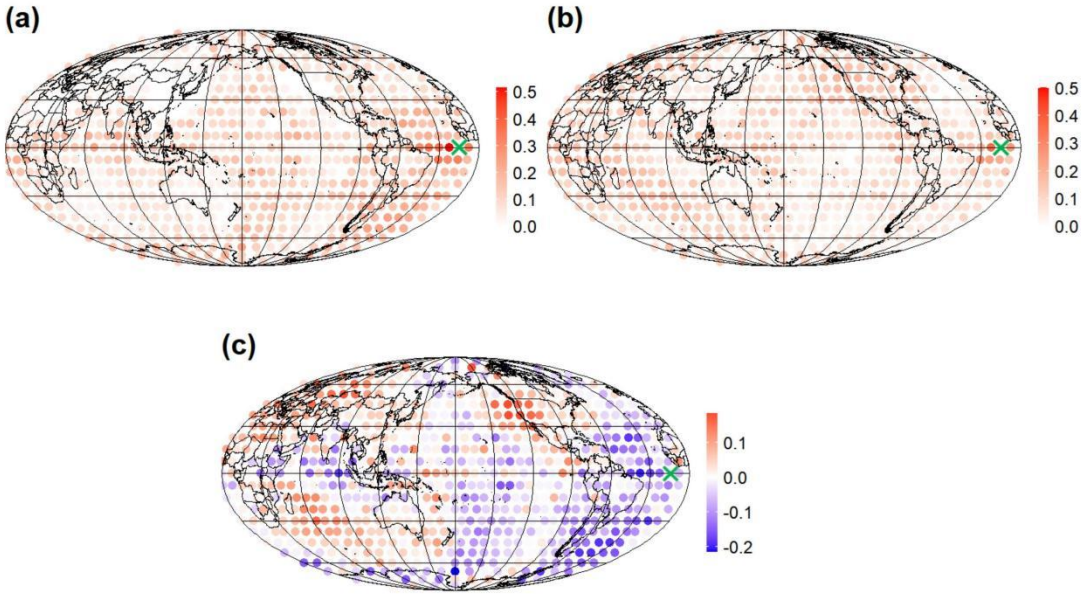

Figure 5: Probability maps of the Atlantic Ocean node and other global nodes belonging to the same community for (a) 1949-1981, (b) 1982-2019, and (c) the difference of the probability between 1982-2019 and 1949-1981. The symbol of cyan cross represents the selected Atlantic Ocean node.

5 Conclusions

In this investigation, we constructed a climate network using near-surface air temperature data spanning from 1949 to 2019. Our aim was to examine the evolution of climate network topology within the context of global warming. To explore how global warming affects the structure of the global climate network, we applied the Louvain community detection algorithm.

Notably, we observed that the network modularity between 1949 and 1981 remained below the overall average, whereas between 1982 and 2019, it exceeded the overall average. Concurrently, the trend in the number of communities from 1949 to 2019 followed a similar pattern to that of modularity. Furthermore, the correlation coefficient between modularity and the number of isolated nodes was

found to be 0.674. Additionally, the correlation between the number of isolated nodes and the number of communities reached 0.929, both of which demonstrated statistical significance. Furthermore, we noted a substantial increase in the number of isolated nodes since 1982. Hence, the shift in modularity and the number of communities since 1982 are significantly associated with the notable surge in the number of isolated nodes. This systematic shift in community structure since the early 1980s could be related to the climate shift and the change of mean state associated with the altered properties of El Niño since the early 1980s (Graham, 1994; Tsonis et al., 2007; Swanson, 2009; Cai et al., 2021; Gan et al., 2023).

Between 1949 and 1981, isolated nodes were sporadic and dispersed, mainly concentrated in the equatorial Pacific and equatorial Atlantic regions. However, from 1982 to 2019, isolated nodes were pervasive across the entire equatorial oceanic region. We further examined the relationship between temperature network structure and isolated nodes in the context of global warming. By selecting key nodes with the highest frequency of isolation in the equatorial Pacific, equatorial Atlantic, and equatorial Indian Ocean regions, we investigated their likelihood of belonging to the same community as other nodes during 1949-1981 and 1982-2019. Our findings suggested that the connectivity of highly isolated nodes along the equator is decreasing, potentially associated with the weakening of tropical circulations such as the Hadley cell and the Walker circulation in response to increasing greenhouse gases. This is particularly notable concerning their associations with neighboring regions within the same oceanic basin. Simultaneously, their connections with certain continents have significantly strengthened.

Data Availability

The data that supports the findings of this study are publicly available online: NCEP/NCAR reanalysis

near-surface (sig995 level) daily air temperature data, https://www.esrl.noaa.gov/psd/data/gridded/data.ncep.reanalysis. derived.surface.html, accessed on 14 September 2022.

Author Contributions

Yi.C.: Investigation, Visualization, Analysis, Writing-Origional draft, Reviewing, Editing. P.Q. : Methodology, Writing, Reviewing, Editing. M.H.: Methodology, Writing, Reviewing, Editing. Yuan.C.: Methodology, Writing, Reviewing, Editing. W.L.: Methodology, Writing, Reviewing, Editing. Y.Z: Investigation, Conceptualization, Analysis, Methodology, Writing, Reviewing, Editing, Supervision.

Competing interests

The contact author has declared that none of the authors has any competing interests.

Disclaimer

Publisher's note: Copernicus Publications remains neutral with regard to jurisdictional claims in published maps and institutional affiliations.

Financial support

This study was supported by the National Natural Science Foundation of China (No. 12305044 and No. 12371460) and the Fundamental Research Program of Yunnan Province (No. CB22052C173A).

References

A.A. Tsonis and K. Swanson: Topology and Predictability of El Niño and La Niña Networks, Phys. Rev. Lett. 100, 228502, https://doi.org/10.1103/PhysRevLett.100.228502, 2008.

A.A. Tsonis, and Paul J. Roebber.: The architecture of the climate network, Physica A, 333: 497-504. https://doi.org/10.1016/j.physa.2003.10.045, 2004.

A.A. Tsonis, K. Swanson, and S. Kravtsov: A new dynamical mechanism for major climate shifts, Geophys, Res. Lett., 34, L13705, https://doi.org/10.1029/2007GL030288, 2007.

A.A. Tsonis, Wang, G., K. Swanson et al.: Community structure and dynamics in climate networks, Clim. Dyn. 37, 933–940, https://doi.org/10.1007/s00382-010-0874-3, 2011.

A.Agarwal, N. Marwan and R. Maheswaran: Quantifying the Roles of Single Stations Within Homogeneous Regions Using Complex Network Analysis, J. Hydrol. 563, S0022169418304724-, https://doi.org/10.1016/j.jhydrol.2018.06.050, 2018.

A.Hunt and P. Watkiss: Climate change impacts and adaptation in cities: a review of the literature, Clim. Change 104, 13–49, https://doi.org/10.1007/s10584-010-9975-6, 2011.

B.F. Christopher, V. Barros, T. F. Stocker and Q. Dahe: Managing the Risks of Extreme Events and Disasters to Advance Climate Change Adaptation: Special Report of the Intergovernmental Panel on Climate Change, CUP: Cambridge, UK , https://doi.org/10.1017/CBO 9781139177245, 2012.

Boers, N., Bedartha Goswami, Aljoscha Rheinwalt, Bodo Bookhagen, Brian Hoskins and Jürgen Kurthsl: Complex networks reveal global pattern of extreme-rainfall teleconnections, Nature 566, 373–377, https://doi.org/10.1038/s41586-018-0872-x, 2019.

Boers, N., Bookhagen, B., Barbosa, H. et al.: Prediction of extreme floods in the eastern Central Andes based on a complex networks approach. Nat. Commun. 5, 5199, https://doi.org/10.1038/ncomms6199, 2014.

Boers, N.: Observation-based early-warning signals for a collapse of the Atlantic Meridional Overturning Circulation, Nat. Clim. Change. 11, 680–688, https://doi.org/10.1038/s41558-021-01097-4, 2021.

Cai, W., Santoso, A., Collins, M. et al.: Changing El Niño – Southern Oscillation in a warming climate, Nat Rev Earth Environ 2, 628 – 644, https://doi.org/10.1038/s43017-021-00199-z, 2021.

Chang, C.-W. J., W.-L. Tseng, H.-H. Hsu, N. Keenlyside, and B.-J. Tsuang: The Madden-Julian Oscillation in a warmer world, Geophys. Res. Lett., 42, 6034 – 6042, https://doi.org/10.1002/2015GL065095, 2015.

Cherifi, H., Palla, G., Szymanski, B.K. et al.: On community structure in complex networks: challenges and opportunities, Appl. Netw. Sci. 4, 117, https://doi.org/10.1007/s41109-019-0238-9, 2019.

Chris D. Thomas, Alison Cameron, Rhys E. Green, Michel Bakkenes, Linda J. Beaumont, Yvonne C. Collingham, Barend F. N. Erasmus, Marinez Ferreira de Siqueira, Alan Grainger, Lee Hannah, Lesley Hughes, Brian Huntley, Albert S. van Jaarsveld, Guy F. Midgley, Lera Miles, Miguel A. Ortega-Huerta, A. Townsend Peterson, Oliver L. Phillips and Stephen E. Williams: Extinction risk from climate

change, Nature 427, 145–148 , https://doi.org/10.1038/nature02121, 2004.

Di Capua, G., Kretschmer, M., Donner, R. V., van den Hurk, B., Vellore, R., Krishnan, R., and Coumou, D.: Tropical and mid-latitude teleconnections interacting with the Indian summer monsoon rainfall: a theory-guided causal effect network approach, Earth Syst. Dynam., 11, 17–34, https://doi.org/10.5194/esd-11-17-2020, 2020.

Emanuel, K.: Increasing destructiveness of tropical cyclones over the past 30 years, Nature 436, 686–688, https://doi.org/10.1038/nature03906, 2005.

Gan, R., Liu, Q., Huang, G. et al.: Greenhouse warming and internal variability increase extreme and central Pacific El Niño frequency since 1980, Nat. Commun. 14, 394, https://doi.org/10.1038/s41467-023-36053-7, 2023.

Graham, N.E.: Decadal-scale climate variability in the tropical and North Pacific during the 1970s and 1980s: observations and model results, Clim. Dyn., 10, 135–162, https://doi.org/10.1007/BF00210626, 1994.

Guez, O. C., Gozolchiani, A. and Havlin, S.: Influence of autocorrelation on the topology of the climate network, Phys. Rev. E, 90(6), 062814, https://doi.org/10.1103/PhysRevE.90.062814, 2014.

Hu K., Huang, G., Huang, P. et al.: Intensification of El Niño-induced atmospheric anomalies under greenhouse warming, Nat. Geosci. 14, 377–382, https://doi.org/10.1038/s41561-021-00730-3, 2021.

I.Salehyan and C.S. Hendrix: Climate shocks and political violence, Glob. Environ. Change 28, 134-145, https://doi.org/10.1016/j.gloenvcha.2014.07.007, 2014.

Intergovernmental Panel on Climate Change (IPCC). Climate Change 2022 – Impacts, Adaptation and Vulnerability: Working Group II Contribution to the Sixth Assessment Report of the Intergovernmental Panel on Climate Change, CUP, https://doi.org/10.1017/9781009325844, 2023.

J. Meng, J. Fan, Y. Ashkenazy, A. Bunde and S. Havlin: Forecasting the Magnitude and Onset of El Niño Based on Climate Network, New J. Phys. 20, 043036, https://doi.org/10.1088/1367-2630/aabb25, 2018.

J.F. Donges, Y. Zou, N. Marwan and J. Kurths: Complex networks in climate dynamics, Eur. Phys. J. Spec. Top. 174, 157–179, https://doi.org/10.1140/epjst/e2009-01098-2, 2009.

J.Fan, J. Meng, Ashkenazy, Y., Havlin, S., Schellnhuber and H.J.: Climate network percolation reveals the expansion and weakeningof the tropical component under global warming, Proc. Natl. Acad. Sci. USA , 115, E12128–E12134, https://doi.org/10.1073/pnas.1811068115, 2018.

J.Fan, J. Meng, J. Ludescher, Zhaoyuan Li, Elena Surovyatkina, Xiaosong Chen, Jürgen Kurths, and Hans Joachim Schellnhuber: Network-based Approach and Climate Change Benefits for Forecasting the Amount of Indian Monsoon Rainfall, Am. Meteorol. Soc.35(3), 1009–1020, https://doi.org/10.1175/JCLI-D-21-0063.1, 2021.

J.Fan, J. Meng, Y. Ashkenazy, S. Havlin and H. J. Schellnhuber: Network Analysis Reveals Strongly Localized Impacts of El Niño, Proc. Natl. Acad. Sci. U.S.A. 114, 7543–7548, https://doi.org/10.1073/pnas.1701214114, 2017.

J.Ludescher, A. Gozolchiani, M. I. Bogachev, A. Bunde, S. Havlin and H. J. Schellnhuber: Very Early Warning of Next El Niño, Proc. Natl. Acad. Sci. U.S.A. 111, 2064–2066, https://doi.org/10.1073/pnas.1323058111, 2014.

J.Ludescher, Martin, M., Boers, N., Bunde, A., Ciemer, C., J.Fan, Havlin, S., Kretschmer, M., Kurths, J., Runge, J.; et al.: Network-based forecasting of climate phenomena, Proc. Natl. Acad. Sci. USA , 118, e1922872118, https://doi.org/10.1073/pnas.1922872118, 2021(a).

K. Swanson, and A. A. Tsonis: Has the climate recently shifted? Geophys. Res. Lett., 36, L06711, https://doi.org/10.1029/2008GL037022, 2009.

K.Yamasaki, A. Gozolchiani, and S. Havlin: Climate Networks around the Globe are Significantly Affected by El Niño, Phys. Rev. Lett. 100, 228501, https://doi.org/10.1103/PhysRevLett.100.228501, 2008.

Kittel, T., Ciemer, C., Lotfi, N. et al.: Evolving climate network perspectives on global surface air temperature effects of ENSO and strong volcanic eruptions, Eur. Phys. J. Spec. Top. 230, 3075–3100 , https://doi.org/10.1140/epjs/s11734-021-00269-9, 2021.

Konapala, G., Mishra, A.K., Wada, Y. et al.: Climate change will affect global water availability through compounding changes in seasonal precipitation and evaporation, Nat Commun 11, 3044 , https://doi.org/10.1038/s41467-020-16757-w, 2020.

Kossin J P, Knapp K R, Olander T L, et al.: Global increase in major tropical cyclone exceedance probability over the past four decades, Proc. Natl. Acad. Sci., 117(22): 11975-11980, https://doi.org/10.1073/pnas.1920849117, 2020.

Lu, J., G. A. Vecchi, and T. Reichler: Expansion of the Hadley cell under global warming, Geophys. Res. Lett., 34, L06805, https://doi.org/10.1029/2006GL028443, 2007.

M.Burke, S. Hsiang, E. and Miguel: Global non-linear effect of temperature on economic production,

391 Nature 527, 235–239, https://doi.org/10.1038/nature15725, 2015.
392 M.E.J. Newman, Mark.: Networks. OUP, 2018.
393 M.E.J. Newman: Modularity and community structure in networks, Proc. Natl. Acad. Sci. 103,
394 8577–8582, https://doi.org/10.1073/pnas.0601602103, 2006.
395 Mondal, S. and Mishra, A. K. : Complex networks reveal heatwave patterns and propagations over the
396 USA, Geophys. Res. Lett., 48, e2020GL090411 , https://doi.org/10.1029/2020GL090411, 2021.
397 Mukherjee, S., Mishra, A. K. : Increase in compound drought and heatwaves in a Warming World,
398 Geophys. Res. Lett., 48(1), e2020GL090617, https://doi.org/10.1029/2020GL090617, 2020.
399 Nordhaus and William D.: Revisiting the social cost of carbon, Proc Natl Acad Sci USA 114(7), 1518,
400 https://doi.org/10.1073/pnas.1609244114, 2017.
401 Palla, G., Derényi, I., Farkas, I. et al.: Uncovering the overlapping community structure of complex
402 networks in nature and society, Nature 435, 814–818, https://doi.org/10.1038/nature03607, 2005.
403 Paluš, M. and Novotná, D.: Northern Hemisphere patterns of phase coherence between
404 solar/geomagnetic activity and NCEP/NCAR and ERA40 near-surface air temperature in period 7–8
405 years oscillatory modes, Nonlin. Processes Geophys., 18, 251–260,
406 https://doi.org/10.5194/npg-18-251-2011, 2011.
407 R.Quian Quiroga, T. Kreuz, and P. Grassberge: Event synchronization: A simple and fast method to
408 measure synchronicity and time delay patterns, Phys. Rev. E 66, 041904,
409 https://doi.org/10.1103/PhysRevE.66.041904, 2002.
410 Rahmstorf, S., Box, J., Feulner, G. et al.: Exceptional twentieth-century slowdown in Atlantic Ocean
411 overturning circulation, Nat. Clim. Change 5, 475 – 480, https://doi.org/10.1038/nclimate2554, 2015.
412 S.Hallegatte, V. Przyluski and A. Vogt-Schilb: Building world narratives for climate change impact,
413 adaptation and vulnerability analyses, Nat. Clim. Change 1, 151–155, https://doi.org/10.1038/
414 nclimate1135, 2011.
415 Scott C Doney , Victoria J Fabry, Richard A Feely and Joan A Kleypas: Ocean Acidification: The
416 Other CO2 Problem, Annu. Rev. Mar. Sci. 1, 169-192,
417 https://doi.org/10.1146/annurev.marine.010908.163834, 2009.
418 Shepherd, T.: Atmospheric circulation as a source of uncertainty in climate change projections, Nat.
419 Geosci.7, 703 – 708 , https://doi.org/10.1038/ngeo2253, 2014.
420 Tantet, A. and Dijkstra, H. A.: An interaction network perspective on the relation between patterns of

421 sea surface temperature variability and global mean surface temperature, Earth Syst. Dynam., 5, 1–14,
422 https://doi.org/10.5194/esd-5-1-2014, 2014.
423 Tokinaga, H., Xie, SP., Deser, C. et al.: Slowdown of the Walker circulation driven by tropical
424 Indo-Pacific warming, Nature 491, 439 – 443, https://doi.org/10.1038/nature11576, 2012.
425 V. D. Blondel, J. L. Guillaume, R. Lambiotte and E. Lefebvre: Fast unfolding of communities in large
426 networks, J. Stat. Mech. 10(10), P10008, https://doi.org/10.1088/1742-5468/2008/10/ P10008, 2008.
427 Vecchi, Gabriel A., and Brian J. Soden: Global Warming and the Weakening of the Tropical
428 Circulation, J. Climate 20(17) : 4316-4340, https://doi.org/10.1175/JCLI4258.1, 2007.
429 Z.Geng, Y. Zhang, B. Lu, J. Fan, Z. Zhao and X. Chen: Network-Synchronization Analysis Reveals the
430 Weakening Tropical Circulations, Geophys. Res. Lett. 48, e2021GL093582,
431 https://doi.org/10.1029/2021GL093582, 2021.
432 Zhang, Y., J.Fan, Chen, X., Ashkenazy, Y., and Havlin, S.: Significant impact of Rossby waves on air
433 pollution detected by network analysis, Geophys. Res. Lett., 46, 12476–12485,
434 https://doi.org/10.1029/2019GL084649, 2019.
435 Zhou, Dong, et al.: Teleconnection Paths via Climate Network Direct Link Detection, Phys. Rev.
436 Lett. 115, 268501, https://doi.org/10.1103/PhysRevLett.115.268501, 2015.
437 Zou, Y., Donner, R. V., Marwan, N., J.F. Donges and Kurths, J.: Complex network approaches to
438 nonlinear time series analysis, Phys. Rep., 787, 1-97.https://doi.org/10.1016/j.physrep.2018.10.005,
439 2019.